Stark resonances and scaling in Rydberg atoms

V. D. Mur,[1)] V. S. Popov, A. V. Sergeev, and A. V. Shcheblykin

Institute of Theoretical and Experimental Physics

(Submitted 7 December 1988)
Zh. Eksp. Teor. Fiz. **96**, 91–106 (July 1989)

The Stark shifts and the widths of highly excited states are calculated in a strong electric field ($n^4\mathscr{E} \sim 1$, $n \gg 1$) for an arbitrary atom (the difference between the atomic field and the Coulomb field is taken into account by introducing quantum defects in a parabolic basis). A correction to the Bohr–Sommerfeld quantization rule, necessitated by the finite barrier penetration factor, is introduced. The possibility of analytic continuation into the above-barrier region is discussed. Scaling relations are obtained via a $1/n$-expansion for the near-threshold Stark resonances with quantum numbers $n_1 \gg 1$, n_2, and $m \sim 1$. The theoretical results are compared with the experimental data on the photoionization of atoms in the presence of a constant electric field $\mathscr{E}$.

1. There are at present numerous experimental results on the near-threshold resonances in the photoionization cross sections of atoms in the presence of a constant electric field $\mathscr{E}$ (see Refs. 1–7 and the citations therein). In Refs. 8 and 9 it was shown that the positions and widths of these resonances coincide with the complex energies $E^{(n_1n_2m)} = E_r - i\Gamma/2$ of the Stark quasistationary states. Various methods have been used to calculate the positions $E_r^{(n_1n_2m)}$ and widths $\Gamma^{(n_1n_2m)}$ of the resonances: summation[10–12] of the divergent perturbation-theory (PT) series and the $1/n$-expansion,[12,13] and also numerical solution of the Schrödinger equation with the radiation condition[8,14] (divergent wave at infinity).

Of greatest interest, from the point of view of experiment, are the states with $n_1 \sim n \gg 1$, n_2 and $m \sim 1$, which have the lowest probability of decay in the field $\mathscr{E}$ (among all the $n(n+1)/2$ Stark sublevels with given n). In this case the $1/n$-expansion is the most adequate method of calculation. However, its use to calculate the widths of the levels raises a peculiar difficulty: within the framework of the $1/n$-expansion the width $\Gamma(\mathscr{E})$ is manifested only in sufficiently strong fields (specifically, after the classical solutions are joined and go off into the complex plane). This difficulty arises not only in problems involving the Stark effect,[13] but also in other problems of quantum mechanics—for example, in problems involving Yukawa and Hulthén potentials.[15] There is always some region near the threshold in which the $1/n$-expansion does not determine the width of the levels.[2)] In the case of the Stark effect this prevents us from joining together the results of the $1/n$-expansion with the well-known (see Refs. 16 and 17, and also the reviews in Refs. 18 and 19) threshold behavior of $\Gamma(\mathscr{E})$ in a weak field. In the present article we show that this difficulty is eliminated if one introduces into the quasiclassical quantization rules a correction for the finite barrier penetration factor.

We briefly describe the contents of this article. Section 2 presents the equations for the energies of the Stark resonances in an arbitrary atom for $n \gg 1$, m (accurate to terms $\sim 1/n^2$ inclusive). Here the deviation of the atomic field from a Coulomb field (for all atoms excluding hydrogen) is taken into account by introducing quantum defects $\delta(n_1n_2m)$ in a parabolic basis. Modification of the quasiclassical quantization rules, taking into account the finite barrier penetration factor is considered in Sec. 3, and the region below the classical ionization threshold in Sec. 4. In Sec. 5, scaling relations for the near-threshold resonances and their consequences are discussed. Finally, in Sections 6 and 7 the results of numerical calculations are discussed and a comparison is made of theory and experiment. The Appendix covers some details of the calculations.

In what follows, unless otherwise specified, we use atomic units and the reduced energy ε and the reduced field F:

$$\varepsilon = \varepsilon' - i\varepsilon'' = 2n^2E^{(n_1n_2m)}, \quad F = n^4\mathscr{E}, \tag{1}$$

n_1, n_2, and m are the parabolic quantum numbers ($m \geqslant 0$), and $n = n_1 + n_2 + m + 1$ is the principal quantum number of the level.

2. **The fundamental equations.** In the calculation of the energy of Rydberg states $|n_1n_2m\rangle$ with $n \gg 1$, m we use the quasiclassical quantization conditions taking into account corrections of order $\hbar^2$ (Ref. 20), the approximate separation of the variables in the parabolic coordinates $\xi = r + z$ and $\eta = r - z$ in the region $r > r_a$ (r_a is the radius of the atomic shell), and the "hidden" symmetry of the Coulomb field,[21,22] which makes it possible to transform from the spherical basis $|nlm\rangle$ to the parabolic $|n_1n_2m\rangle$. To determine ε and the separation constants β_i ($\beta_1 + \beta_2 = 1$) we derive the equations

$$\begin{aligned} &\beta_1(-\varepsilon)^{-1/2}f(z_1) - (F/8n^2)(-\varepsilon)^{-3/2}[g(z_1) - m^2h(z_1)] = \nu_1, \\ &\beta_2(-\varepsilon)^{-1/2}f(z_2) + (F/8n^2)(-\varepsilon)^{-3/2}[g(z_2) - m^2h(z_2)] = \nu_2, \end{aligned} \tag{2}$$

where

$$z_i = (-1)^i 16\beta_i F/\varepsilon^2, \quad \nu_i = (1-\delta/n)[n_i + (m+1)/2]/n, \tag{3}$$

$i = 1$ or 2, the parameter $\delta = \delta(n_1n_2m)$ is expressed in terms of the quantum defects μ_l for a free ($\mathscr{E} = 0$) atom:

$$\delta(n_1n_2m) = \frac{1}{n}\sum_{l=m}^{n-1}(2l+1)\,(C^{JM}_{J,M-m;lm})^2\mu_l, \tag{4}$$

$$J = (n-1)/2, \quad M = (n_1 - n_2 + m)/2 = J - n_2,$$

and $f(z)$, $g(z)$, and $h(z)$ are expressed in terms of the hypergeometric function $F(z) \equiv {}_2F_1(\alpha,\beta;\gamma;z)$:

$$\begin{aligned} f(z) &= F(1/4, 3/4; 2; z), \\ g(z) &= 1/3F(3/4, 5/4; 2; z) + 2/3F(3/4, 5/4; 1; z), \\ h(z) &= F(3/4, 5/4; 2; z) \end{aligned} \tag{5}$$

 0038-5646/89/070049-09$04.00

[in the derivation of formulas (5) we have used Kummer's quadratic transformation,[23] which greatly simplifies the answer]. These equations (for $m = 0$) have already been used before[9]; their derivation is given in Ref. 24. We note that the corrections not taken into account in Eqs. (2) are of order not greater than n^{-4}, so that the accuracy of system (2) in the case of Rydberg states is quite high.

In the weak ($F \to 0$) field region, using the expansion of the functions $f(z)$, $g(z)$, and $h(z)$ for small z, we obtain from Eqs. (2) the expansions

$$\begin{aligned}\varepsilon^{(n_1 n_2 0)} = &-1+3\varkappa F-{}^1/_8(17-3\varkappa^2+19n^{-2})F^2\\ &+{}^3/_{16}\varkappa(23-\varkappa^2+39n^{-2})F^3\\ &-(2\delta/n)[1+3\varkappa F-{}^1/_8(42+35n^{-2})F^2\\ &+{}^{15}/_{32}\varkappa(47-3\varkappa^2+65n^{-2})F^3]+O(F^4, n^{-4}, \delta^2),\end{aligned} \tag{6}$$

$$\begin{aligned}\beta_1 = &{}^1/_2(1+\varkappa)+{}^1/_8[3(1-\varkappa^2)+n^{-2}]F+{}^1/_{16}\varkappa(1-\varkappa^2+6n^{-2})F^2\\ &+{}^1/_{256}(171-186\varkappa^2+15\varkappa^4+622n^{-2}-390\varkappa^2n^{-2}+55n^{-4})F^3\\ &-(\delta/n)\left\{\frac{3}{8}[5(1-\varkappa^2)+n^{-2}]F+{}^{39}/_{16}\varkappa n^{-2}F^2\right.\\ &+{}^3/_{256}(745-830\varkappa^2+85\varkappa^4\\ &\left.+2306n^{-2}-1506\varkappa^2n^{-2})F^3\right\}+\ldots,\end{aligned}$$

which for $\delta = 0$ coincide with the well-known[16,18] perturbation-theory expansions (here $m = 0$, $\varkappa = (n_1 - n_2)/n$, and β_2 is obtained by making the substitution $\varkappa \to -\varkappa$, $F \to -F$). For arbitrary F Eqs. (2) were solved numerically.

Before considering the results of the numerical calculations, we will investigate system (2) qualitatively. Here we omit terms of order $1/n^2$, as a result of which only the function $f(z)$ remains in Eqs. (2). We will call such an approximation a $1/n$-approximation, and the solution of the complete system — a $1/n^2$-approximation. The variable z_1 decreases with growth of F, remaining negative all the time, while z_2 grows; as long as $z_2 < 1$ the solution (i.e., ε, β_1, and β_2) remains real. At $z_2 = 1$ a singularity of the function $f(z)$ is reached, after which the solution departs to the complex plane. The value $F = F_*$, at which $z_2 = 1$, we shall call the classical ionization threshold [in the limit $n \to \infty$ it corresponds to the vanishing of the barrier in the effective potential[16] $U_2(\eta)$].

Setting $z_2 = 1$ in system (2) taken in the $1/n$-approximation, we arrive at the equation

$$tf(-t) = (2^{7/2}/3\pi)(2n/p-1), \tag{7}$$

which does not depend on the quantum defect δ. Here

$$\begin{aligned}&p = 2n_2+m+1, \quad \beta_1 = t(1+t)^{-1}, \quad \beta_2 = (1+t)^{-1},\\ &F_* = (2^{7/2}n/3\pi p)^4(1+t)^{-3}.\end{aligned} \tag{7'}$$

Numerical solution of this equation gives the curve $\mu = 0$ in Fig. 1.

We calculated F_* for all the states in which one of the numbers $\varkappa_1$, $\varkappa_2$, or μ vanishes in the limit $n \to \infty$ ($\varkappa_i = (n_i + 1/2)/n$, $\mu = m/n$). The results are presented in Fig. 1. The values of F_* for an arbitrary state $|n_1 n_2 m\rangle$ lie inside the curvilinear triangle in Fig. 1 (see also Ref. 25).

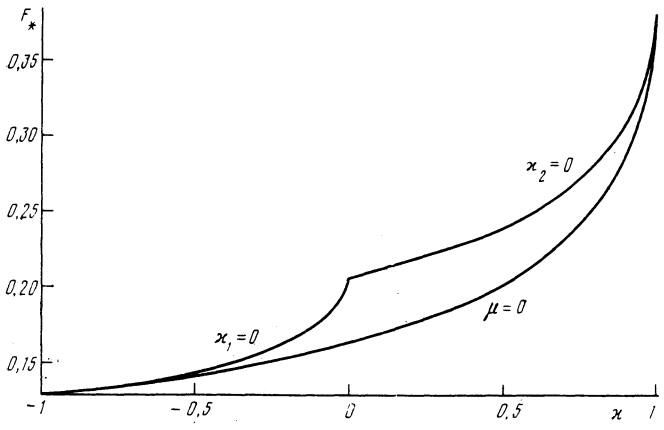

FIG. 1. Classical ionization threshold F_* for three series of states; $\varkappa = \varkappa_1 - \varkappa_2 = (n_1 - n_2)/n$.

Figure 2 shows values of F_* for a few series of states which are of experimental interest ($n_1 \gg n_2$ and m, $p = 1$–5). With growth of p the value of F_* markedly decreases, which is reflected in the width of the atomic levels—see Table II below.

As long as $F < F_*$ the solution of system (2) remains real and does not describe the width of the atomic levels in that region where ionization has a tunneling character (here, however, the position of the levels is calculated with high accuracy—see Sec. 5 below). To overcome this difficulty we consider quantization conditions which take account of the finite-barrier-penetration factor.

3. As is well known,[16] for the potential $V(\mathbf{r}) = -r^{-1} - \mathscr{E}z$ the variables in the Schrödinger equation separate in the parabolic coordinates ξ, η, φ:

$$\psi(\mathbf{r}) = N(\xi\eta)^{-1/2}\chi_1(\xi)\chi_2(\eta)e^{im\varphi}. \tag{8}$$

After transforming to the reduced variables ε, F, and $y = n^{-2}\eta$, the equation for χ_2 takes the form

$$\begin{aligned}&\frac{d^2\chi_2}{dy^2}+\left[p^2(y)+\frac{1}{4y^2}\right]\chi_2 = 0,\\ &p(y) = n\left(\frac{\varepsilon}{4}+\frac{\beta_2}{y}-\frac{\mu^2}{4y^2}+\frac{Fy}{4}\right)^{1/2}.\end{aligned} \tag{9}$$

In the classically allowed region

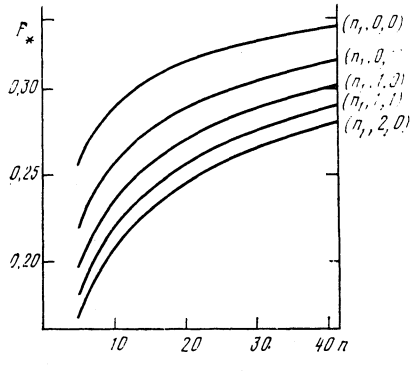

FIG. 2. The dependence of F_* on n (the parabolic quantum numbers are shown for each curve).

$$\chi_2 \propto [p(y)]^{-1/2} \sin[\theta(y)+\pi/4], \quad y_0<y<y_1, \tag{10}$$

and according to Langer's method, with allowance for the correction of order $\hbar^2$ to the quasiclassical approximation,[20] the phase $\theta(y)$ is equal to

$$\theta(y)=\int_{u_0}^{u} du\left[Q-\frac{1}{4}\frac{d}{du}\left(\frac{1}{Q^2}\frac{dQ}{du}\right)-\frac{1}{8Q^3}\left(\frac{dQ}{du}\right)^2\right],$$

$$u=\ln y, \quad Q(u)=e^u p(e^u).$$

Returning to the variable y, we have accurate to terms of order $1/n^2$

$$\theta(y)=\int_{y_0}^{y} dy\left\{p-\frac{1}{4}\left(\frac{p'}{p^2}\right)'-\frac{p'^2}{8p^3}+\frac{1}{8py^2}\right\}, \tag{10'}$$

where the prime denotes the derivative with respect to y. The quasiclassical solution (10) is inapplicable when the turning points $y_{1,2}$ are close to the top of the potential barrier

$$y=y_{max}=2(\beta_2/F)^{1/4}-\mu^2/4\beta_2+\ldots.$$

For $m=0$, setting $y=y_{\max}(1+\alpha\rho)$ and $\alpha=(F/64n^4\beta_2^3)^{1/8}$, we reduce Eq. (9) in the region $|\rho|\ll(\beta_2^3/F)^{1/8}$ to standard form[23]:

$$\frac{d^2\chi_2}{d\rho^2}+\left(\frac{\rho^2}{4}-a\right)\chi_2=0, \quad a=-n\left(\frac{\beta_2}{64F^3}\right)^{1/4}[\varepsilon+4(\beta_2 F)^{1/2}]. \tag{11}$$

In the general case, when the energy E is not necessarily close to the top of the barrier in $U_2(\eta)$,

$$a=\frac{1}{\pi}\int_{\eta_1}^{\eta_2}(-p_\eta^2)^{1/2}\,d\eta, \quad p_\eta^2=-\left(\frac{m^2}{4\eta^2}-\frac{\beta_2}{\eta}-\frac{1}{4}\mathscr{E}\eta-\frac{1}{2}E\right) \tag{12}$$

($\eta_{1,2}$ are the turning points, $\eta_1<\eta<\eta_2$ is the below-barrier region). For the states with $m=0$ this integral can be calculated analytically:

$$a=[n(-\varepsilon)^{1/4}/2^{7/2}F](1-z_2)f(1-z_2), \tag{13}$$

where $z_2=16\beta_2 F/\varepsilon^2$, and $f(z)$ is given by Eq. (5). The barrier vanishes when $\varepsilon=-4(\beta_2 F)^{1/2}$ and $z_2=1$ ($\alpha=0$). It is not difficult to see that (13) goes over to (11) as $z_2\to 1$.

To the left of the barrier the solution of Eq. (11), corresponding to the quasistationary state (divergent wave as $\rho\to\infty$), takes the form[3)]

$$\chi_2 \propto [\tau(1-2a/\tau^2)]^{-1/2}\sin[\theta(\tau)+\pi/4], \tag{14}$$

where

$$\theta(\tau)=\frac{1}{4}\tau^2-a\ln\tau+\frac{1}{4i}\ln\left[\frac{\Gamma(1/2+ia)}{\Gamma(1/2-ia)(1+e^{-2\pi a})}\right]+\frac{1}{2}\left(a^2-\frac{3}{4}\right)\tau^{-2}+\ldots, \quad \tau=-\rho\gg|a|.$$

The quantization condition arises from the requirement of coincidence of functions (10) and (14) in the overlap region $|a|\ll\tau\ll n^{1/2}(\beta_2^3/F)^{1/8}$, which always exists for large n. In this case we make the substitution $p=(\tau^2/4-a)^{1/2}$ (the parabolic approximation, $y\approx y_{\max}$) and go over in the complex y plane to a contour integral which includes the points $y=y_0$ and $y=y_1(\tau=2a^{1/2})$. We finally come to system (2), in which it is necessary to make in the second equation the substitution:

$$n_2\to n_2-\varphi(a)/2\pi \tag{15}$$

[for n_1 such a substitution is not necessary since the potential $U_1(\xi)$ is a barrier potential for all $F>0$]. Here in the $1/n$-approximation

$$\varphi(a)\equiv\varphi_1=\frac{1}{2i}\ln\left[\frac{\Gamma(1/2+ia)}{\Gamma(1/2-ia)(1+e^{-2\pi a})}\right]-a\ln a+a, \tag{16}$$

and in the $1/n^2$-approximation, i.e., taking into account in system (2) terms which are proportional to $F/8n^2$,

$$\varphi(a)\equiv\varphi_2(a)=\varphi_1(a)-1/24a \tag{16'}$$

(the properties of these functions are considered in Appendix A). Let us now discuss these formulas.

a) For $F\ll F_*$ Eqs. (2) with allowance for substitution (15) give the correct threshold behavior of the widths of the atomic levels in a weak field (see the next Section).

b) For $F\ll F_*$ the solution of system (2) becomes complex. The singularity at $F_*=F_*$ can be avoided by choosing the correct sign $\operatorname{Im} E=-\Gamma/2<0$:

$$f(z_2)\to f(z_2)-2^{1/2}i(1-z_2)F(5/4, 7/4; 2; 1-z_2). \tag{17}$$

On the other hand, taking into account the asymptotic limit (A2) (see Appendix A), substitution (15) takes the form

$$\nu_2\to\nu_2+ia/n, \tag{18}$$

which is consistent with substitution (17) for $|1-z_2|\ll 1$. Hence it follows that analytic continuation of the Bohr–Sommerfeld quantization rules from the region of the quasidiscrete spectrum to the above-barrier region determines both the position and the width of the levels (far from the complex turning points). This explains a fact which was previously established empirically,[13,15] namely that the $1/n$-expansion, even without account of the penetrability of the barrier, allows one to calculate the width of the quasistationary states in a strong field (after the joining of the two classical solutions).

c) The function (16) has singularities at the points

$$a=a_n=(n+1/2)i, \quad n=0, 1, 2, \ldots, \tag{19}$$

which correspond to the poles of the amplitude of scattering by the parabolic barrier $V(x)=-\omega^2x^2/2$. In this case

$$\psi=\text{const}\, D_{-ia-1/2}(2^{1/2}e^{-i\pi/4}\xi)=\begin{cases}(-\xi)^{ia-1/2}e^{-i\xi^2/2}+A(-\xi)^{-ia-1/2}e^{i\xi^2/2}, & \xi\to-\infty,\\ B\xi^{-ia-1/2}e^{i\xi^2/2}, & \xi\to+\infty,\end{cases}$$

where

$$x=(\hbar/m\omega)^{1/2}\xi, \quad a=-E/\omega, \quad \hbar=m=1.$$

The amplitudes of the reflected (A) and transmitted (B) waves

$$B=ie^{-\pi a}A=(2\pi)^{-1/2}2^{-ia}e^{\pi a/2}\Gamma(1/2+ia) \tag{20}$$

have poles at $a=a_n$, where $E=E_n=-i(n+1/2)\omega$, and the wave functions are given by

$$\psi_n(\xi)=\text{const}\, e^{i\xi^2/2}H_n(\xi e^{-i\pi/4})\propto\xi^n e^{i\xi^2/2}, \quad \xi\to\pm\infty.$$

(We note that the substitution $\omega \to i\omega$ transforms the parabolic barrier into a harmonic-oscillator potential, and the energy values $E = E_n$ correspond to oscillator's energy spectrum.) On the other hand, the existence of the poles A and B at the mirror points $a = a_n^* = -(n + 1/2)i$ would contradict the Hermitian character of the Hamiltonian: then there would exist square-integrable ($n \geqslant 0$) wave functions

$$\psi_n(\xi) \propto \xi^{-ia-1/2} e^{i\xi^2/2} = \xi^{-(n+1)} e^{i\xi^2/2}, \quad \xi \to \pm\infty,$$

corresponding to complex energy eigenvalues $E = E_n^*$.

d) The effect of the penetrability of the barrier on the quasiclassical quantization rules were considered by Rice and Good,[26] Drukarev,[27] and Kondratovich and Ostrovskiĭ.[28] The expressions in Refs. 26 and 27 for the correction to the quantization rules correspond to

$$\varphi(a) = \arg \Gamma(1/2 + ia) + a(1 - \ln a),$$

which is practically identical to Eq. (16) for real $a \gg 1$. However, as the level approaches the apex of the barrier this expression becomes inaccurate. In particular, the function $\varphi(a)$ would in this case have singularities not only at $a = a_n$, but also the points $a = a_n^*$, which do not correspond to poles of the scattering amplitude.

4. **The weak field region.** Using the perturbation-theory expansion (6), we find from Eq. (12)

$$2\pi a = n\{2/3F + (1-\varkappa)\ln F - [1 + 2\ln 2 + 2\varkappa(1 - \ln 2) - \lambda_+ \ln \lambda_+ - \lambda_- \ln \lambda_-] + \ldots\}, \quad (21)$$

where

$$\lambda_\pm = (1 - \varkappa \pm \mu)/2, \quad \varkappa = (n_1 - n_2)/n, \quad \mu = m/n$$

(here $0 < \lambda_- \leqslant \lambda_+ < 1$) and the terms which vanish as $F \to 0$ have been omitted. Taking Eq. (A4) into account, we see that Eqs. (2) go over into the usual quantization rules accurate to terms of order $1/n^2$ if we work in the $1/n$-approximation, and to terms of order $1/n^4$ in the $1/n^2$-approximation (see also item 4) of Appendix A). A new feature is the appearance of an imaginary part, albeit exponentially small, in n_2: $\operatorname{Im} n_2 = -(4\pi)^{-1} \exp(-2\pi a)$. Setting $E = E_r - i\Gamma/2$, we arrive from the condition

$$\int_{q_1}^{q_2} p\, dq = (n + 1/2)\pi$$

at the Gamow formula for the level width:

$$\Gamma = T^{-1} e^{-2\pi a}, \quad T = 2\int_{q_1}^{q_2} p^{-1}\, dq, \quad (22)$$

where T is the period of the oscillations of the classical particle.

The problem of the Stark effect in the hydrogen atom does not reduce to a one-dimensional problem. In this case the quasiclassical formula is

$$\tilde{\Gamma}^{(n_1 n_2 m)} = \frac{\sigma_1}{(\sigma_1 \tau_2 + \sigma_2 \tau_1) n^3} e^{-2\pi a}, \quad (23)$$

where

$$2\pi a = n \int_{y_1}^{y_2} |k_2(y)|\, dy,$$

$$\sigma_1 = \int_{x_0}^{x_1} \frac{dx}{x k_1(x)}, \quad \tau_1 = \int_{x_0}^{x_1} \frac{dx}{k_1(x)}, \quad (23')$$

$$\sigma_2 = \int_{y_0}^{y_1} \frac{dy}{y k_2(y)}, \quad \tau_2 = \int_{y_0}^{y_1} \frac{dy}{k_2(y)}$$

(see Appendix B). Here we assume that $n \gg 1$ and we make the scaling transformation

$$\xi = n^2 x, \quad \eta = n^2 y, \quad p_\xi = k_1(x)/2n, \quad p_\eta = k_2(y)/2n, \quad (24)$$

so that

$$k_1^2 = \varepsilon - Fx + 4\beta_1/x - \mu^2/x^2, \quad k_2^2 = \varepsilon + Fy + 4\beta_2/y - \mu^2/y^2. \quad (25)$$

As $F \to 0$ formula (23) takes the form

$$\tilde{\Gamma}^{(n_1 n_2 m)}(\mathscr{E}) = (2\pi n^3)^{-1} e^{-2\pi a} \propto F^{-p} e^{-2n/3F}, \quad p = 2n_2 + m + 1. \quad (26)$$

[see Eqs. (21) and (B4)], which functionally coincides with the exact asymptotic limit[16,17] of the width $\Gamma^{(n_1 n_2 m)}(\mathscr{E})$ as $\mathscr{E} \to 0$, differing only by a numerical factor in the pre-exponential factor. We note that approximation (26) possesses good accuracy even for not large quantum numbers. Thus, $R_{n_1 n_2 m} \equiv \tilde{\Gamma}^{(n_1 n_2 m)}/\Gamma^{(n_1 n_2 m)} = 0.865$, 0.905, and 0.947, respectively, for the ground state $|0,0,0\rangle$ and the states $|0,0,1\rangle$ and $|0,1,0\rangle$, and for $n_2 \gg 1$

$$R_{n_1 n_2 m} = 1 - (2n_2 + m)/24 n_2 (n_2 + m) + \ldots \to 1.$$

Thus, taking account of the penetrability of the barrier in the quasiclassical quantization rules gives the correct behavior of the widths of the atomic levels in a weak field.

5. Numerical solution of system (2) with account of the substitution (15) gives a reasonable interpolation between the weak field region and the "scaling" region $F > F_*$. Typical results, in the instance of the state $|19,0,0\rangle$ in the hydrogen atom, are presented in Fig. 3 of Ref. 30. Correction (15) is very important for $F \lesssim F_*$, but with further growth of the field its role decreases (as can be seen from Fig. 3, for $F > 1.25F_*$, even without taking the penetrability of the barrier into account, the $1/n$-approximation determines the width of the level with sufficient accuracy).

As to the effect of the penetrability of the barrier on the position $E_r^{(n_1 n_2 m)}$ of the quasistationary level, it is not large. For example, $\varepsilon_n' = 2n^2 E_r^{(n-1,0,0)} = -0.1508$ and -0.1574 without taking account of the penetrability of the barrier, while $\varepsilon_n' = -0.1490$ and -0.1488 with this account (for $n = 20$ and $F = 0.35$; here the first number corresponds to the $1/n$-approximation, the second to the $1/n^2$-approximation). It can be seen that introducing correction (15) stabilizes the calculated values of ε_n', and determines the energy with accuracy of the order of 10^{-4}. This allows us to limit ourselves in the majority of cases to the solution of Eqs. (2) and (15) in the $1/n$-approximation.

Numerical calculations of the energy levels and widths were carried out for the hydrogen atom by Damburg and Kolosov.[29] We have calculated the values of $\nu = (-2E_r)^{1/2}$ and Γ by two independent methods: 1) summation of the perturbation-theory series with the help of Padé–Hermite approximants, and 2) solution of Eqs. (2) in the $1/n$- and $1/n^2$-approximations. The results for the states with $n_1 = n_2 = (n-1)/2$ and $m = 0$ along with the corre-

TABLE I.

(n_1, n_2, m) / $\mathscr{E}$ / F	(2,2,0), $n=5$ 1,8 (−4) 0,1125		(5,5,0), $n=11$ 1,0 (−5) 0,1464		(7,7,0), $n=15$ 3,0 (−6) 0,1519	
Method of calculation	ν	Γ	ν	Γ	ν	Γ
PHA [12]	4,92402	2,283(−6)	10,713	2,83(−6)	14,577	1,35(−6)
$1/n$	4.92385	2.22(−6)	10,7128	2,82(−6)	14.5767	1.347(−6)
$1/n^2$	4.92406	2,19(−6)	10.7127	2,80(−6)	14.5766	1.338(−6)
[29]	4.9240	2,282(−6)	10.688	2,815(−6)	14.5771	1.338(−6)

sponding values from Ref. 29 are listed in Table I. The agreement of all the calculations is quite good, which confirms the method of summation of divergent PT series (for the Stark effect) which we have chosen and permits one to use the Padé–Hermite approximants and Eqs. (2) for still stronger fields.

6. **Scaling for near-threshold resonances.**[4)] Let $n\to\infty$ and n_2/n, $m/n\to 0$. In this limit the system (2) reduces to one equation:

$$(-\varepsilon)^{1/2}=F(1/4;\ 3/4;\ 2;\ -16F\varepsilon^{-2}), \tag{27}$$

whose solution we denote by $\varepsilon_{\rm cl}(F)$. Using the $1/n$-expansion,[13] it is possible to show that for the states with $n_1\sim n\gg 1$, n_2 and $m\sim 1$ the following relations are satisfied: for $E>0$

$$E_r^{(n_1n_2m)}=\frac{1}{2\tilde{n}^2}\varepsilon_{cl}(\tilde{n}^4\mathscr{E}),\quad \Gamma^{(n_1n_2m)}=\frac{pn_*}{n\tilde{n}^3}\gamma_{cl}(\tilde{n}^4\mathscr{E}), \tag{28}$$

and in the below-threshold energy region $E<0$

$$E_r^{(n_1n_2m)}=(1/2\tilde{n}^2)\,[\varepsilon_{cl}(\tilde{n}^4\mathscr{E})+\eta((\tilde{n}n_*)^2\mathscr{E})-(\tilde{n}/n_*)^2\eta(n_*^4\mathscr{E})]. \tag{29}$$

Here $\tilde{n}=n_1+(m+1)/2-\delta$, $n_*=n-\delta$ (the analog of the effective principal quantum number $n-\mu_l$, which is introduced[16] for Rydberg states in the spherical basis $|nlm\rangle$), $\delta=\delta(n_1n_2m)$, $p=2n_2+m+1$, and the functions $\gamma_{\rm cl}(F)$ and $\eta(F)$ are expressed in terms of $\varepsilon_{\rm cl}(F)$—see Ref. 30 and Appendix C. These equations give definite scaling laws for the Stark resonances and are accurate to order $1/n^2$ (see Appendix C).

We point out a number of consequences of these scaling relations.

a) As a rule, in an experiment the field $\mathscr{E}$ is fixed and a set of resonances with given n_2 and m is observed. In this case the principal quantum number n corresponding to the intersection of the Stark level with the boundary of the ionization limit $E=0$ is equal to

$$n=n^{(0)}=37{,}5\mathscr{E}^{-1/4}+n_2+(m+1)/2+\delta,$$

and the slope of the level at the point of intersection is equal to

$$\left.\frac{d\varepsilon_{n_1n_2m}}{dF}\right|_{\varepsilon'=0}=\frac{3\pi}{4}\left[1-\left(n_2+\frac{m+1}{2}+\delta\right)\frac{1}{n}+O\left(\frac{1}{n^2}\right)\right]. \tag{30}$$

With growth of p the slope decreases, in agreement with numerical calculations.[12]

b) In the hydrogen atom the reduced energies $\varepsilon'_{n_1n_2m}$ of the states $|n-2,1,0\rangle$ and $|n-3,0,2\rangle$ are extraordinarily close to each other (see Fig. 1 in Ref. 9 for $n=25$); the same holds, although with less accuracy, for $\varepsilon''_{n_1n_2m}=n^2\Gamma^{(n_1n_2m)}$. The explanation of this result follows from Eqs. (28): the states under discussion have the same values of p and $\tilde{n}=n-p/2$ ($n_*=n$ for hydrogen), wherefore the positions and the widths of the resonances differ (for given $\mathscr{E}$) only in terms of order $1/n^2$. The same is true for the states $|n-3,1,1\rangle$ and $|n-4,0,3\rangle$; $|n-3,2,0\rangle$, $|n-4,1,2\rangle$, and $|n-5,0,4\rangle$; etc. (as long as $p\ll n$).

On the other hand, for the states $|n-m-1,0,m\rangle$ we have $\tilde{n}=n-(m+1)/2$, wherefore ε' and ε'' differ already in terms of order $1/n$.

c) For the hydrogen atom all $\delta\equiv 0$, and $\tilde{n}$ does not depend on n_2. Therefore the positions of the above-threshold resonances with fixed n_1 and m but different n_2 should be close to each other, with their widths proportional to p (see also Ref. 28). For example,

$$\Gamma^{(n_100)}(\mathscr{E}):\Gamma^{(n_110)}(\mathscr{E}):\Gamma^{(n_120)}(\mathscr{E})\approx 1:3:5. \tag{31}$$

d) The width of the peaks in the region $E>0$ increase rapidly with the energy of the resonance. The condition $\Gamma\approx\Delta E$ allows one to estimate the value $n=n_c$ at which neighboring resonances overlap and the structure in the photoionization cross sections vanishes. Using Eqs. (28) and the linear approximation for $\varepsilon_{\rm cl}(F)$, we find

$$n_c=k_c\mathscr{E}^{-1/4}+n_2+(m+1)/2+\delta, \tag{32}$$

where $k_c=0.787(1+x_0)^{1/4}$, and x_0 is a root of the equation

$$x[(1+x/3)/(1+x/2)]^2=2p^{-2}.$$

For the numer of peaks which can be observed in the above-threshold region, we obtain the estimate $\Delta n=n_c-n^{(0)}\mathscr{E}k_1\mathscr{E}^{-1/4}$, $k_1=0.332$, 0.095, and 0.043 for $p=1$,2, and 3. The structure in the photoionization cross sections is most noticeable for the states $|n_1,0,0\rangle$, and with growth of p the number of peaks Δn falls off rapidly. For example, for a hydrogen atom in a field $\mathscr{E}=8.0$ kV/cm we have $\Delta n\approx 9$ for the series $|n_1,0,0\rangle$ and $\Delta n\approx 1$ for $|n_1,1,0\rangle$.

7. **Comparison with experiment.** Reference 6 gives the positions and widths of the below-threshold ($E<0$) Stark resonances with $m=0$ in the hydrogen atom. These numbers are in good agreement both with calculations based on Eq. (2) in the $1/n$-approximation (taking into account the penetrability of the barrier) and with the results of the summation of the perturbation-theory series (see Table II, which gives the values of $E_r^{(n_1n_2m)}$ taken with the opposite sign, and $\Gamma/2$). Here the error in the experimental energies E_r can reach 2 cm^{-1} (see Ref. 6).

As can be seen from Table II, the widths $\Gamma^{(n_1n_2m)}$ at first

TABLE II.

H ($\mathscr{E}$ = 16,8 kV/cm

n_1n_2m	F_*	$-E_r$, cm^{-1}		$\Gamma/2$, cm^{-1}		f
		theory	expt. (Ref. 6)	theory	expt. (Ref. 6)	
16,1,0	0,2654	106.6	103,8	8.9	9.0	0.292
16,0,0	0,3096	123,3	126,5	0.15	0.14	−0.119
15,1,0	0,2626	167.6	167.9	1.9	2.1	0,039
15,0,0	0,3074	196.7	198.5	7.0(−4)	1.1(−4)	−0,303
14,2,0	0,2362	211,5	210.1	5.6	6.6	0,155
13,2,0	0,2329	274.2	275.9	0.27	0.23	−0,081
12,3,0	0,2143	313.8	314.8	1.3	1.6	−0,001
11,4,0	0,2001	352.2	351.4	3.3	3.0	0.070
11,3,0	0,2107	384,4	386.3	1.9(−3)	1.8(−3)	−0.215
10,4,0	0.1965	419.1	419.2	2.5(−2)	3.2(−2)	−0,158

Rb ($\mathscr{E}$ = 2.189 kV/cm				Na ($\mathscr{E}$ = 3,59 kV/cm			
n_1n_2m	δ	$-E_r$, cm^{-1}		n_1n_2m	δ	$-E_r$, cm^{-1}	
		theory	expt. (Ref. 1)			theory	expt. (Ref. 3)
23,0,0	0.656	132.8	133	26,0,0	0.140	15.5	15.5
22,0,0	0.681	157.1	157±2	25,0,1	0,0073	21.1	21.5
21,1,0	0.517	159.5	160	25,0,0	0.145	35.5	35.5
20,2,0	0.400	163.2	163	24,0,1	0.0078	40.4	41
21,0,0	0.708	184.2	185	24,1,0	0.130	50.3	50.5
20,1,0	0.531	185.4	185	24,0,0	0.151	57.0	56.5
20,0,0	0.737	214.6	217±2	23,0,1	0.0085	60,7	61
18,1,0	0.561	247.2	247	23,0,0	0.157	80.3	79
16,2,0	0.428	284.0	284	22,0,1	0.0092	83.1	84
18,0,0	0.802	288.6	289	22,1,1	0.016	74.9	75

glance vary irregularly, although the resonances are arranged in order of decreasing E_r. This apparent irregularity is explained if we compare $F = n^4\mathscr{E}$ with the classical ionization threshold $F_*(n_1n_2m)$; there is a distinct correlation between the quantities $\Gamma/2$ and $f = (F - F_*)/F_*$ (the latter characterizes the closeness of the resonance energy to the top of the potential barrier).

Table II also gives the values of $-E_r$ for rubidium and sodium. The experimental data were taken from the graphs in Refs. 1 and 3 and have an accuracy of ~ 1 cm^{-1} (as the resonances begin to overlap, the accuracy decreases), within the limits of which the theory agrees with experiment. Here it is important to take into account the quantum defect δ in Eqs. 2, particularly in the case of rubidium.[5] Similar results were also obtained for other states. More detailed tables given in Ref. 31 include around 50 states $|n_1n_2m\rangle$ with $m = 0$ and 1. In all cases the positions of the resonances agree to within several percent; for $\Gamma^{(n_1n_2m)}$ the agreement between theory and experiment is somewhat poorer, but at the present time even the widths have not been determined experimentally at so high an accuracy.

In Ref. 30 it has been shown that scaling relation (28) is satisfied for $E > 0$. Let us turn now to the below threshold resonances. The experimental values of the energy $E_r^{(n_1n_2m)}$ taken from Refs. 1, 3, 5, and 6 were scaled and shifted in the following way:

$$\tilde{\varepsilon}_{n_1n_2m} = 2\tilde{n}^2E_r^{(n_1n_2m)} - \eta((\tilde{n}n_*)^2\mathscr{E}) + (\tilde{n}/n_*)^2\eta(n_*^4\mathscr{E}). \quad (33)$$

If Eq. (29) is satisfied, the values $\tilde{\varepsilon}_{(n_1n_2m)}$ plotted versus $\tilde{F} = \tilde{n}^4\mathscr{E}$ should lie on a universal curve $\varepsilon_{cl}(\tilde{F})$ regardless of the atom under consideration. As can be seen from Fig. 3, this is indeed the case. We note that the points corresponding to fixed n and $n_2 = 0,1,\ldots,4$ agree within the limits of accuracy of the figure, which is in accord with statement c) in Sec. 6.

As to the widths of the resonances, for $F \gtrsim 0.5$ the experimental points lie on a universal curve based on Eq. (28)

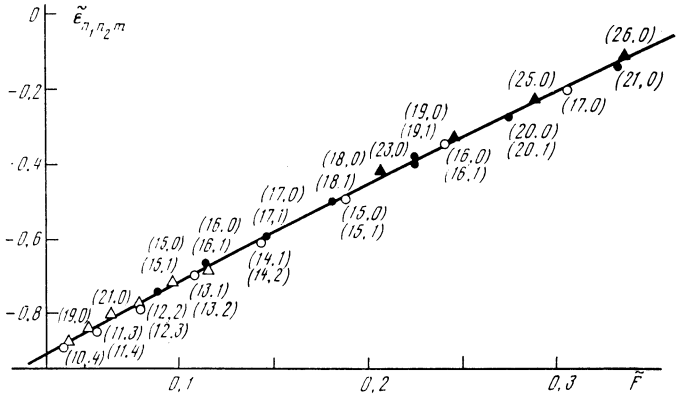

FIG. 3. Verification of scaling relation (29) for the below-threshold Stark resonances. For each experimental point its quantum numbers (n_1 and n_2) are indicated; for all states $m = 0$. The solid curve is $\tilde{\varepsilon}_{cl}(F)$. Symbols: ○—the states $|n_1,n_2,m\rangle$ in the hydrogen atom (Ref. 6) for $\mathscr{E} = 16.8$ kV/cm ($10 \leqslant n_1 \leqslant 17$, $0 \leqslant n_2 \leqslant 4$); ●—the states $|n_1,n_2,m\rangle$ in hydrogen (Refs. 4 and 5) for $\mathscr{E} = 8.0$ kV/cm ($n_1 = 15$–21, $n_2 = 0$ and 1); ▲—the states $|n_1,0,0\rangle$ in the sodium atom (Ref. 3) for $\mathscr{E} = 3.59$ kV/cm and $n_1 = 23$–26; △—the states $|n_1,0,0\rangle$ for rubidium (Ref. 1) for $\mathscr{E} = 2.189$ kV/cm and $n_1 = 19$–24.

[see Fig. 4)]. In this figure the field $\tilde{F} = \tilde{n}^4\mathscr{E}$ is the abscissa, and the quantities

$$\tilde{\gamma}_{n_1n_2m} = (n\tilde{n}^3/pn_*)\Gamma^{(n_1n_2m)}(\mathscr{E}), \quad p = 2n_2 + m + 1. \tag{34}$$

are the ordinates.

For $F < 0.4$ deviations from scaling are observed and are due to the finite penetrability of the barrier. The numerical solution of Eq. (2) is in agreement with experiment, as can be seen from Table II. Here the term with $\varphi(a)$ in (15) plays in the region $F > F_*$ a comparatively small role, in agreement with the remarks in Sec. 3.

8. The number of experimental points in Figs. 3 and 4 could be easily increased. The agreement is good in all of the cases which we have considered, and undoubtedly the observed peaks in the photoionization cross sections correspond to the Stark quasistationary states. The scaling relations (28) and (29) can be used to describe Rydberg states close to $E = 0$ for any atom. These relations are suitable both as a test of numerical calculations and to identify the quantum numbers (n_1n_2m) of the peaks in photoionization spectra.

The authors express their sincere appreciation to V. M. Vainberg, B. M. Karnakov, E. A. Solov'ev, and especially to L. P. Pitaevskiĭ for a discussion of results and helpful remarks:

APPENDIX A

We list some properties of the function $\varphi(a)$.

1) The behavior at large radius:

$$\varphi(a) \approx \begin{cases} \sum_{k=1}^{\infty} c_k a^{-(2k-1)}, & -\pi < \arg a < \frac{\pi}{2}, \quad \text{(A1)} \\ -2\pi i a + \sum_{k=1}^{\infty} c_k a^{-(2k-1)}, & \frac{\pi}{2} < \arg a < \pi, \quad \text{(A2)} \end{cases}$$

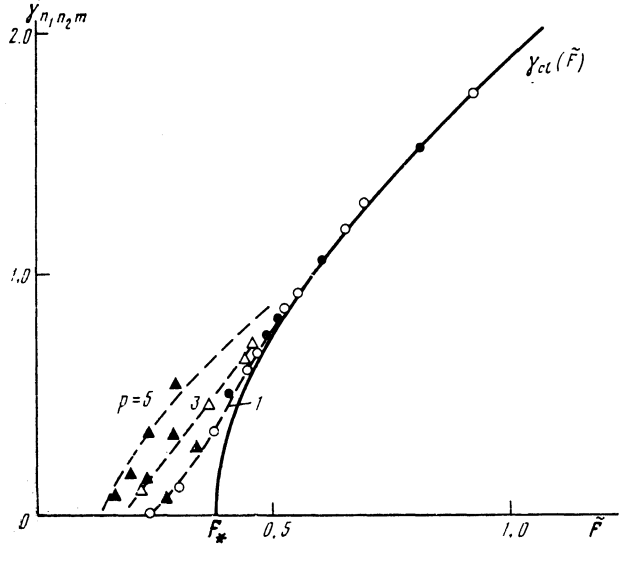

FIG. 4. Scaling for the widths of the Stark resonances: ○, ●, and △—the states $(n_1,0,0)$, $(n_1,0,1)$, and $(n_1,1,0)$ in the hydrogen atom for $\mathscr{E} = 6.5$ and 8.0 kV/cm (Ref. 5); ▲—the states $(n_1,n_2,0)$ with $n_2 = 0,1,2$ (correspondingly $p = 1,3,5$) for sodium for $\mathscr{E} = 3.59$ kV/cm (Ref. 3); $F_* = 0.383$—see Eq. (C9).

where

$$c_k = (-1)^{k-1}(1-2^{1-2k})B_{2k}/2k(2k-1), \quad |a| \to \infty$$

and B_{2k} are the Bernoulli numbers. These series diverge although the coefficients c_k decrease initially: $c_1 = 1/24$, $c_2 = 7/2880$,... (the smallest coefficient is $c_4 = 5.906 \cdot 10^{-4}$; for $k \gg 1$ these coefficients grow factorially).

2) On the real axis we have

$$\operatorname{Im} \varphi(a) = {}^1/_2 \ln(1+e^{-2\pi a}), \quad 0 < a < \infty, \tag{A3}$$

$$\varphi(a) = 1/24a + \ldots + {}^1/_2 i \exp(-2\pi a), \quad a \to +\infty \tag{A4}$$

3) $\varphi(a)$ has logarithmic branch points at $a = 0$ (where it remains finite) and at the points (19):

$$\varphi(a) = i \ln(a - a_n) + O(1), \quad a \to a_n. \tag{A5}$$

At the points $a = a_n^*$ this function is regular since the limit

$$\lim_{a \to a_n^*} \Gamma({}^1/_2 - ia)(1+e^{-2\pi a}) = 2\pi i^{2n+1}/n! \tag{A6}$$

has a finite value. For this reason the amplitudes (20) do not have any singularities in this case.

The properties of the function $\varphi(a)$ are considered in detail in Ref. 31.

4) The preceding formulas pertain to the function $\varphi(a)$ introduced in Eq. (16). For the $1/n^2$-approximation, Eq. (16') should be used; in this case the first term in Eq. (A1) is canceled and the expansion begins with $c_2 a^{-3}$. Apparently allowance for the succeeding corrections[20] to the quasiclassical approximation, up to $\hbar^{2K}$ inclusive, leads to the function

$$\varphi_K(a) = \varphi(a) - \sum_{k=1}^{K-1} c_k a^{-(2k-1)}, \tag{A7}$$

for which $\varphi_K(a) = O(a^{-(2K-1)})$ as $a \to \infty$. As can be seen from Eqs. (2), the formal parameter $\hbar^2$ of the quasiclassical expansion for the energy is equal here to $1/n^2$. Therefore substitution in (15) of the function φ_K for φ should ensure a relative accuracy of order n^{-2K} in the quantization rules (for the position of the level E_r). For $K = 1$ and 2 this is the case.

APPENDIX B

In the derivation of the pre-exponential factor in Eq. (23) we have used the quasiclassical approximation. Since the normalization of the wave function (8) is carried out in the classically allowed region $\xi_0 < \xi < \xi_1$, $\eta_0 < \eta < \eta_1$, we have

$$N = [{}^1/_2\pi(\sigma_1\tau_2 + \sigma_2\tau_1)]^{-1/2} n^{-2}, \tag{B1}$$

where σ_i and τ_i are defined by Eqs. (23'). Recognizing that the barrier exists only for the variable η, we obtain

$$\chi_2(\eta) = \begin{cases} p_\eta^{-1/2} \cos\left(\int_\eta^{\eta_1} p_\eta\, d\eta - \frac{\pi}{4}\right), & \eta_0 < \eta < \eta_1, \\ \frac{1}{2} e^{-\pi a} \exp\left\{i\left(\int_{\eta_2}^{\eta} p_\eta\, d\eta + \frac{\pi}{4}\right)\right\}, & \eta > \eta_2, \end{cases}$$

where the parameter a is defined by Eq. (12). Calculating the flux of the particles escaping to infinity, we arrive at Eq.

(23). Formulas of this type can be obtained also for other problems with separable variables.

In the limit as $F \to 0$ we have

$$\sigma_1=\sigma_2=\pi, \quad \tau_i=2\pi\beta_i^{(0)}=2\pi[n_i+{}^1/_2(m+1)]/n, \tag{B2}$$

therefore in Eq. (23) the pre-exponential factor has the form $T^{-1}(0) = 1/2\pi n^3$, which is in agreement with the Gamow formula [for bounded motion in a Coulomb field we have $T = 2\pi(-2E)^{-3/2} = 2\pi n^3$ according to Kepler's third law].

For the states with $m = 0$ the integrals in Eqs. (23) can be calculated analytically:

$$\begin{aligned}\sigma_i&=\pi(-\varepsilon)^{-1/2}F({}^1/_4;\ {}^3/_4;\ 1;\ z_i),\\ \tau_i&=2\pi\beta_i(-\varepsilon)^{-1/2}F({}^3/_4;\ {}^5/_4;\ 2;\ z_i)\end{aligned} \tag{B3}$$

[the variables z_i are defined in Eqs. (2)]. Hence

$$T^{-1}=[1-{}^3/_2(1-\varkappa)F-{}^3/_8(17+\varkappa-2\varkappa^2)F^2+\ldots]/2\pi n^3, \tag{B4}$$

in particular, $T^{-1} = (1 - 6F^2 + \ldots)/2\pi n^3$ for the states $|n_1,0,0\rangle$ with $n_1 \gg 1$.

The second case, in which the pre-exponential factor is easily calculated, is that of the state $|0,0,m\rangle$ with $m = n - 1 \gg 1$. With the help of the $1/n$-expansion we obtain

$$T^{-1}=(1-3\tau)^{1/2}(1+\tau)/2\pi n^3(1-\tau), \tag{B5}$$

where[13] $\tau(1-\tau^2)^4 = F$, with $\tau = \tau(F) \to 0$ as $F \to 0$ and for $0 < \tau < 1/3$.

We note, finally, that for a short-range potential $\beta_i \to 0$ and, according to Eq. (13),

$$2\pi a=\pi\varkappa^3 f(1)/2^{5/2}F=2\varkappa^3/3F. \tag{B6}$$

Therefore, in this case Eq. (26) gives the correct exponential[32] in the probability of ionization of the s-level ($n = 1$, $E = \varepsilon/2 = -\varkappa^2/2$).

APPENDIX C
Derivation of the scaling relations

We observe that the substitutions

$$F \to \mu^{-1}F, \quad \varepsilon \to \mu^{-1/2}\varepsilon, \quad n \to \mu^{-1/4}n, \quad \beta_i \to \beta_i$$

do not change the values $z_{1,2}$, and the left-hand sides of Eqs. (2) acquire a common factor $\mu^{1/4}$. Choosing $\mu = (1 - \delta/n)^4$, we can eliminate δ and transform to the "hydrogen" variables $\bar{\varepsilon}$, $\bar{F}$, and $\bar{n} = n_*$:

$$\bar{\varepsilon}=\mu^{-1/2}\varepsilon=2n_*^2E, \quad \bar{F}=\mu F=n_*^4\mathscr{E}, \quad \bar{n}=\mu^{1/4}n=n-\delta. \tag{C1}$$

Since

$$\bar{\nu}_i=[\bar{n}_i+{}^1/_2(m+1)]/\bar{n}=[n_i+{}^1/_2(m+1)]/n\equiv\nu_i,$$

($\bar{n}_i = n_i - \delta$), the right-hand sides of Eqs. (2) have the same value as for the state $|n_1n_2m\rangle$ in the hydrogen atom ($\delta = 0$).

Now let $n_1 \gg n_2, m$. The position of the Stark resonances in the region $E > 0$ is determined primarily by the first of Eqs. (2), which follows from the quantization condition in the coordinate ξ. Recognizing that $\nu_1 = 1 - p/2n$, $p = 2n_2 + m + 1$, we obtain in analogy with Eqs. (C1) the result that the scaling transformation

$$\operatorname{Re}\bar{\varepsilon}=\rho^{-1/2}\varepsilon_{cl}(\rho\bar{F}), \quad \rho=(1-p/2n)^4 \tag{C2}$$

reduces the problem to the limiting case $n \to \infty$. Combining Eqs. (C1) and (C2), we find the final form of the scaling factor $\lambda = \mu\rho$:

$$\lambda=\left\{1-\frac{1}{n}[n_2+(m+1)/2+\delta]\right\}^4, \tag{C3}$$

where $\delta = \delta(n_1n_2m)$.

To obtain the scaling relations we use the $1/n$-expansion:

$$\begin{aligned}\varepsilon=\varepsilon_0+\frac{p}{n}\varepsilon_1+\frac{1}{n^2}(p^2\varepsilon_2+\xi_2+m^2\eta_2)\\ +\frac{1}{n^3}(p^3\varepsilon_3+p\xi_3+m^2p\eta_3)+\ldots,\end{aligned} \tag{C4}$$

where $\varepsilon_0 = \varepsilon_{cl}(F)$ is the solution of Eq. (27) (we have taken account of the fact that Eqs. (2) contain three small parameters: $\nu_2 = p/2n$, $1/n^2$, and m^2/n^2). Successive expansion of Eqs. (2) in powers of $1/n$ demonstrates that

$$\varepsilon_1=(1-2Fd/dF)\varepsilon+(1-Fd/dF)(-\varepsilon)^{1/2}, \tag{C5}$$

$$\operatorname{Im}\varepsilon_2={}^3/_2\varepsilon^{1/2}[\varepsilon-{}^3/_2F\dot{\varepsilon}+\varepsilon^{-1}(F\dot{\varepsilon})^2+2F^2\ddot{\varepsilon}], \quad F>F_*, \tag{C6}$$

$$\xi_2=\frac{F^2}{24\varepsilon(\varepsilon-2F\dot{\varepsilon})^2}[19\varepsilon^2\dot{\varepsilon}+48F\varepsilon\dot{\varepsilon}^2+36F^2\dot{\varepsilon}^3+8F\varepsilon^2\ddot{\varepsilon}],$$

where for brevity we have written $\varepsilon \equiv \varepsilon_0$, $\dot{\varepsilon} = d\varepsilon_0/dF$, etc.

The functions ε_0, ξ_2, and η_2 remain real for all $0 < F < \infty$, but ε_1 and ε_2 each acquires an imaginary part if $F > F_*$. Indeed, using the Kummer transformation[23] for the hypergeometric function, Eq. (27) can be rewritten in parametric form ($-1 \leqslant u < 1$):

$$\begin{aligned}\varepsilon_{cl}&=4F^{1/2}u(1-u^2)^{-1/2},\\ F^{1/4}&={}^1/_2(1-u^2)^{1/4}{}_2F_1({}^1/_2;\ {}^5/_2;\ 2;\ (1+u)/2)),\end{aligned}$$

from which it is clear that the function $\varepsilon_{cl}(F)$ is real for all $F > 0$. It follows from Eq. (C6) that the same is also true for $\xi_2(F)$. The absence of an imaginary part in ξ_2 and η_2 was also checked by summation of the corresponding PT series.

For $F > F_*$ the first term in Eq. (C5) contributes to the real part, and the second term—to the imaginary part of the correction to ε_1. Hence

$$\begin{aligned}\varepsilon'_{n_1n_2m}\equiv 2n^2E_r^{(n_1n_2m)}&=\varepsilon_{cl}+(p/n)(1-2Fd/dF)\varepsilon_{cl}+\ldots\\ &=\rho^{-1/2}\varepsilon_{cl}(\rho F)+O(1/n^2),\end{aligned} \tag{C7}$$

$$\begin{aligned}\varepsilon''_{n_1n_2m}=n^2\Gamma^{(n_1n_2m)}&=-\operatorname{Im}\left(\frac{p}{n}\varepsilon_1+\frac{p^2}{n^2}\varepsilon_2+\ldots\right)\\ &=\frac{p}{n}\rho^{-3/4}\gamma_{cl}(\rho F)+O\left(\frac{1}{n^3}\right).\end{aligned}$$

In the below-threshold region $\varepsilon_1(F)$ is real. The same is also true for the subsequent terms in Eq. (C4); therefore in this case the $1/n$-expansion only determines the position of the level, but not its width (an analogous situation occurs for the Yukawa and Hulthén potentials[15]). Proceeding as in the foregoing and taking formulas (C1)–(C3) into account, we find

$$\varepsilon'_{n_1n_2m}=\lambda^{-1/2}\varepsilon_{cl}(\lambda F)+\lambda^{-1/2}\eta((\lambda\mu)^{1/2}F)-\mu^{-1/2}\eta(\mu F). \tag{C8}$$

Transforming from ε to the energy E, we obtain the scaling relations (28) and (29). Since the two first (nonvanishing) terms of the $1/n$-expansion were used in their derivation, their relative accuracy is of the order of $1/n^2$.

Let us determine the introduced functions γ_{cl} and η. For $F > F_* = 0.3834$ we have

$$\gamma_{cl}(F) = \varepsilon^{1/2}(^3/_2 F\dot{\varepsilon} - \varepsilon) = (Fd/dF - 1)\,[\varepsilon_{cl}(F)]^{1/2}, \qquad (C9)$$

and for $F < F_*$ and $\varepsilon_{cl}(F) < 0$

$$\eta(F) = [-\varepsilon_{cl}(F)]^{1/2}. \qquad (C10)$$

The $\varepsilon_{cl}(F)$ curve intersects the ionization limit $E = 0$ at $F = F_*$:

$$\varepsilon_{cl} = \alpha_1 f + \alpha_2 f^2 + \ldots, \quad f = (F - F_*)/F_*, \qquad (C11)$$

where $\alpha_1 = 0.9034$, $\alpha_2 = -0.0673$, $\alpha_3 = 0.0173$, $\alpha_4 = -0.0063$,..., i.e., $\alpha_1 \gg |\alpha_2| > \alpha_3$. This explains the approximate linearity of the ε_{cl} curve (F), which is conspicuously distinct in Fig. 3. We note that the function $\varepsilon_{cl}(F)$ is real for $0 < F < \infty$ and has no singularities for $F = F_*$, while $\gamma_{cl}(F)$ has a square-root singularity here.

[1)]Moscow Engineering-Physics Institute.
[2)]See Fig. 2 in Ref. 15 for the Yukawa potential and Fig. 3 in Ref. 13 for the Stark effect in the hydrogen atom.
[3)]See the Darwin expansion (Ref. 23) for the parabolic cylinder function $W(\alpha,\tau)$.
[4)]A brief presentation of the results of this section was published earlier.[30]
[5)]For fixed n the quantum defects $\delta(n_1 n_2 m)$ decay with growth of n_2 and, in particular, with growth of the magnetic quantum number m [see Eq. (4)]. As estimates we give the following numbers ($n = 25$, the rubidium atom): $\delta(24, 0, 0) = 0.633$, $\delta(23, 1, 0) = 0.491$, $\delta(22, 2, 0) = 0.386$, $\delta(22, 1, 1) = 0.133$, $\delta(23, 0, 1) = 0.092$, and $\delta(22, 0, 2) = 0.0067$. For hydrogen $\delta \equiv 0$ for all states.

[1]R. R. Freeman and N. P. Economou, Phys. Ref. **A20**, 2356 (1979).
[2]W. Sandner, K. A. Safinya, and T. F. Gallagher, Phys. Rev. **A23**, 2448 (1981).
[3]T. S. Luk, L. DiMauro, T. Bergeman *et al.*, Phys. Rev. Lett. **47**, 83 (1981).
[4]W. L. Glab and M. N. Nayfeh, Phys. Rev. **A31**, 530 (1985).
[5]W. L. Glab, K. Ng, D. Yao, and M. N. Nayfeh, Phys. Rev. **A31**, 3677 (1985).
[6]K. Ng, D. Yao, and M. N. Nayfeh, Phys. Rev. **A35**, 2508 (1987).
[7]D. Yao, K. Ng, and M. N. Nayfeh, Phys. Rev. **A36**, 4072 (1987).
[8]V. V. Kolosov, Pis'ma v Zh. Eksp. Teor. Fiz. **44**, 457 (1986) [JETP Lett. **44**, 588 (1986)].
[9]V. M. Vaĭnberg, V. D. Mur, V. S. Popov, and A. V. Sergeev, Pis'ma v Zh. Eksp. Teor. Fiz. **46**, 178 (1987) [JETP Lett. **46**, 225 (1987)].
[10]L. Benassi and V. Grecchi, J. Phys. **B13**, 911 (1980).
[11]V. Franceschini, V. Grecchi, and H. J. Silverstone, Phys. Rev. **A32**, 1338 (1985).
[12]V. M. Vaĭnberg, V. D. Mur, V. S. Popov, and A. V. Sergeev, Pis'ma v Zh. Eksp. Teor. Fiz. **44**, 9 (1986) [JETP Lett. **44**, 9 (1986)]; Zh. Eksp. Teor. Fiz. **93**, 450 (1987) [Sov. Phys. JETP **66**, 258 (1987)].
[13]V. S. Popov, V. D. Mur, A. V. Shcheblykin, and V. M. Weinberg, Preprint ITEP. 86-125, 1986; Phys. Lett. **A124**, 77 (1987).
[14]V. V. Kolosov, J. Phys. **B20**, 2359 (1987).
[15]V. S. Popov, V. M. Vainberg, and V. D. Mur, Pis'ma v Zh. Eksp. Teor. Fiz. **41**, 439 (1985) [JETP Lett. **41**, 539 (1985)]; Yad. Fiz. **44**, 1103 (1986) [Sov. J. Nucl. Phys. **44**, 714 (1986)].
[16]L. D. Landau and E. M. Lifshitz, *Quantum Mechanics* (*Nonrelativistic Theory*) Pergamon, 1978.
[17]T. Yamabe, A. Tachibana, and H. J. Silverstone, Phys. Rev. **A16**, 877 (1977).
[18]R. J. Damburg and V. V. Kolosov, *Rydberg States of Atoms and Molecules*, Cambridge Univ. Press, Cambridge (1983), p. 42.
[19]V. S. Lisitsa, Uspekh. Fiz. Nauk **153**, 379 (1987) [Sov. Phys. Usp. **30**, 927 (1987)].
[20]J. D. Bekenstein and J. B. Krieger, Phys. Rev. **188**, 130 (1969).
[21]V. A. Fock, Z. Phys. **98**, 145 (1935).
[22]D. Park, Z. Phys. **159**, 155 (1960).
[23]M. Abramowitz and I. Stegun, *Handbook of Mathematical Functions*, U. S. Govt. Printing Office, Washington (1972).
[24]V. D. Mur and V. S. Popov, Preprint ITÉF 93-89, 1989.
[25]M. B. Kadomtsev and B. M. Smirnov, Zh. Eksp. Teor. Fiz. **80**, 1715 (1981) [Sov. Phys. JETP **53**, 885 (1981)].
[26]M. H. Rice and R. H. Good, J. Opt. Soc. Amer. **52**, 239 (1962).
[27]G. F. Drukarev, Zh. Eksp. Teor. Fiz. **75**, 473 (1978) [Sov. Phys. JETP **48**, 237 (1978)].
[28]V. D. Kondratovich and V. N. Ostrovsky, J. Phys. **B17**, 1981, 2011 (1984).
[29]R. J. Damburg and V. V. Kolosov, J. Phys. **B9**, 3149 (1976); **B11**, 1921 (1978); **B12**, 2637 (1979).
[30]V. D. Mur and V. S. Popov, Pis'ma v Zh. Eksp. Teor. Fiz. **48**, 67 (1988) [JETP Lett. **48**, 70 (1988)].
[31]V. D. Mur, V. S. Popov, and A. V. Sergeev, Preprint ITÉF-18, 1988; V. S. Popov, V. D. Mur, A. V. Sergeev *et al.*, Preprint ITEP N 61-89, 1989.
[32]Yu. N. Demkov and G. F. Drukarev, Zh. Eksp. Teor. Fiz. **47**, 918 (1964) [Sov. Phys. JETP **20**, 614 (1965)].

Translated by Paul Schippnick